

# Model reproduces individual, group and collective dynamics of human contact networks

Michele Starnini,<sup>1</sup> Andrea Baronchelli,<sup>2</sup> and Romualdo Pastor-Satorras<sup>1</sup>

<sup>1</sup>*Departament de Física i Enginyeria Nuclear, Universitat Politècnica de Catalunya, Campus Nord B4, 08034 Barcelona, Spain*

<sup>2</sup>*Department of Mathematics, City University London, Northampton Square, London EC1V 0HB, UK*

Empirical data on the dynamics of human face-to-face interactions across a variety of social venues have recently revealed a number of context-independent structural and temporal properties of human contact networks. This universality suggests that some basic mechanisms may be responsible for the unfolding of human interactions in the physical space. Here we discuss a simple model that reproduces the empirical distributions for the individual, group and collective dynamics of face-to-face contact networks. The model describes agents that move randomly in a two-dimensional space and tend to stop when meeting ‘attractive’ peers, and reproduces accurately the empirical distributions.

## I. INTRODUCTION

Social and Cognitive Sciences have experienced a major transformation in the past few years [8, 37, 63]. The recent availability of large amounts of data has indeed fostered the quantitative understanding of many phenomena that had previously been considered only from a qualitative point of view [7, 33]. Examples range from human mobility patterns [12] and human behavior in economic arenas [48, 49], to the analysis of political trends [2, 15, 36]. Together with the World-Wide Web, a wide array of technologies have also contributed to this data deluge, such as mobile phones or GPS devices [22, 40, 59], radio-frequency identification devices [16], or expressly designed online experiments [17]. The understanding of social networks has clearly benefitted from this trend [33]. Different large social networks, such as mobile phone [46] or email [11] communication networks, have been characterized in detail while the rise of online social networks has provided an ideal playground for researchers in the social sciences [23, 31, 35]. The availability of data, finally, has allowed to test the validity of the different models of social networks that have mainly been published within the physics-oriented complex networks literature, bridging the gap between mathematical speculations and the social sciences [60].

Among the different kinds of social networks, a prominent position is occupied by the so-called face-to-face contact networks, which represent a pivotal substrate for the transmission of ideas [44], the creation of social bonds [58], and the spreading of infectious diseases [38, 52]. The uniqueness of these networks stems from the fact that face-to-face conversation is considered the “gold standard” [42] of communication [18, 34], and although it can be costly [27], the benefits it contributes to workplace efficiency or in sustaining social relationships are so far unsurpassed by the economic convenience of other forms of communication [42]. It is because face-to-face interactions bring about the richest information transfer [20], for example, that in our era of new technological advancements business travel has kept increasing so steadily [42]. In light of all this, it is not surprising that face-to-

face interaction networks have long been the focus of a major attention [4, 5, 10], but the lack of fine-grained and time-resolved data represented a serious obstacle to the quantitative comprehension of the dynamics of human contacts. Researchers in social network analysis had in fact long pointed out the importance of the temporal dimension for the understanding of social networks, which are not static entities, but rather vary in time [14, 21, 41].

Recently, the so-called data revolution has invested also the study of human face-to-face contact networks [1, 57]. In particular, the fine-grained measurement of face-to-face interactions using wearable active radio-frequency identification devices (RFID), performed by the SocioPatterns collaboration [1], revealed the complex temporal and structural properties of human contact networks [16]. Important among these properties is the bursty nature of human social contacts [6], revealed in the distributions of the time of contact between pairs of individuals, the total time spent in contacts by a given individual, or the inter-event times between consecutive contacts involving the same individual, all exhibiting heavy tails, more or less compatible with a power-law form [16, 54]. The fact that these statistical regularities are common to such apparently diverse settings as schools, hospitals, scientific conferences, and museums, suggests that the properties of human face-to-face contact networks can be explained by some fundamental, general process, independently from the considered situation, and calls for simple models to explain and reproduce these features [32, 65].

In this paper we present and analyze a simple model able to replicate most of the main statistical regularities exhibited by human face-to-face contact networks data. The key insight of the model is the suggestion that the social “attraction” of individuals may be the major responsible for the observed phenomenology of face-to-face contact networks. This insight is implemented by allowing individuals, each characterized by an intrinsic social *attractiveness*, to wander randomly in a two dimensional space—representing the simplified location of a social gathering—until they meet someone, at which point they have the possibility of stopping and starting

a “face-to-face” interaction. Without entering into the problem of the definition of attractiveness, we adopt here an operative approach: Attractive individuals are more likely to make people stop around them and start an interaction, but they are also more prone to abandon their interactions if these are initiated by less attractive agents.

We observe that these simple rules, and the asymmetry of the interactions that they imply, are sufficient to reproduce quantitatively the most important features of the empirical data on contact networks. We explore in particular properties belonging to three different scales. At the *individual, or ‘microscopic’, level*, we focus in temporal properties related to the distributions of contact durations or inter-contact times, and in structural properties related to the time integrated representation of the contact data, as usually reported in the literature [33]. A preliminary account of the model results at this level was presented in Ref. [55]. Moving beyond the analysis of individual properties, we consider here the *group, or ‘mesoscopic’, level*, represented by groups of simultaneously interacting individuals, which typify a crucial signature of face-to-face networks [4, 5] and have important consequences on processes such as decision making and problem solving [13]. We measure the distribution of group sizes as well as the distribution of duration of groups of different size. We finally zoom one more step out and inspect the *collective, or ‘macroscopic’, level* looking at properties that depend on the time interaction pattern of the whole population. We address in particular the issue of the causality patterns of the temporal network, as determined by the time-respecting paths between individuals [29, 41] and the network reachability, defined as the minimum time for information to flow from an individual  $i$  to another individual  $j$  and measured by means of a searching process performed by a random walker [41, 47, 54]. We observe that the model reproduces not only qualitatively, but also quantitatively, the properties measured from empirical data at all the scales.

Finally, as a check for robustness, we explore the role of the parameters that define the model. Particular emphasis is made on the motion rule adopted by the individuals. While a simple random walk for the individuals’ movements is initially considered, in fact, a consistent amount of literature suggests that Lévy flights [61] might provide a better characterization of human movement [9, 12, 24, 50]. We observe that the results of the model are robust with respect to various possible alterations of the original formulation, including the adopted rule of motion.

The paper is structured as follows: In Section II we discuss the SocioPatterns experiment, and present the time-varying network formalism used to represent its data. The model is defined in detail in Section III, while Section IV, Section V and Section VI, address the model behavior concerning the individual, group and collective dynamics, respectively. In Section VII we show the model robustness with respect to the variation of the main parameters involved. Finally, Section VIII is devoted to

discussion, with particular attention to the crucial role of social attractiveness in the model.

## II. EMPIRICAL DATA

### A. The SocioPatterns experiment

Here we consider the data on human contact networks as recorded by the SocioPatterns collaboration [1] in closed gatherings of individuals, covering scientific conferences, hospital wards, and schools. In the deployments of the SocioPatterns infrastructure, each individual participating in the experiment wears a badge equipped with an active radio-frequency identification (RFID) device, able to relay the information about the close proximity of other devices. The emissions of the RFIDs are of low frequency and power, and highly directional. Thus, the close proximity registered by two devices can be associated to their respective wearers being face to face at a short distance, a fact that can be assumed to correspond to a conversation taking place among them. The devices properties are tuned so that face-to-face interactions are recorded with a space resolution of 1 – 2 meters and a time resolution  $\Delta t_0 \sim 20$  seconds, representing the elementary time interval in the contact network evolution.

We will contrast numerical simulations of the proposed model against empirical results from SocioPatterns deployments in several different social contexts: a Lyon hospital (“Hospital”), the Hypertext 2009 conference (“Conference”), the Société Française d’Hygiène Hospitalière congress (“Congress”) and a high school (“School”). A further description of these datasets can be found in [16, 19, 32, 56].

### B. Face-to-face networks as time-varying graphs

The empirical data collected by the SocioPatterns deployments are naturally described in terms of temporally evolving graphs (temporal networks) [30, 41], whose nodes are defined by a static collection of individuals, and whose links represent pairwise interactions, which appear and disappear over time. Interactions between individuals are aggregated over a time window  $\Delta t_0 = 20$ s, corresponding to the natural resolution of the RFID devices. Thus, all the interactions established within this time interval are considered as simultaneous and contribute to build a “instantaneous” contact network, formed by isolated nodes and small groups of interacting individuals. Therefore, each dataset consists of a time-varying network with a number  $N$  of different interacting individuals and a total duration of  $T$  elementary time steps. This procedure is standard in the study of time-varying networks, and represents a tractable and good approximation as far as the aggregation window is not too large [51].

An exact representation of temporal networks is given in terms of a *contact sequence*, representing the sequence of contacts (edges) as a function of time. This sequence is expressed by a characteristic function [43],  $X(i, j, t)$ , taking the value 1 when nodes  $i$  and  $j$  are connected at time  $t$ , and zero otherwise, for  $t \in [0, T]$ . The temporal patterns of the contact sequence can be statistically characterized as its most basic (individual) level by the distribution of the duration  $\Delta t$  of contacts (conversations) between pairs of individuals,  $P(\Delta t)$ , and the distribution of gap times,  $\tau$ , between two consecutive conversations involving a common individual and two other different individuals,  $P(\tau)$ .

A coarse-grained view of temporal networks can be obtained by means of a projection into an aggregated static network, integrated over the whole observation time  $T$ . The edges in the integrated networks indicate the presence of a contact between two nodes at any point in the past. One key variable that characterizes the topology of the network is the degree of a node  $k_i$ , is associated to the total number of different contacts node  $i$  has had during the integration time  $T$ , which can be interpreted as a measure of social integration [39] or activity [62]. Edges can be additionally classified according to their importance or role (eg., family, friends, work colleagues, acquaintances) [25, 64], and heterogeneities in links can be revealed also in the specific case of face-to-face networks. In particular, each edge is annotated with a weight  $w_{ij}$ , indicating the total time spent in interactions by the pair of nodes  $i$  and  $j$ , and which is defined by

$$w_{ij} = \frac{1}{T} \sum_t X(i, j, t). \quad (1)$$

The strength of node  $i$ , defined as  $s_i = \sum_j w_{ij}$ , expresses then the cumulative time spent in interactions by individual  $i$  [32, 46, 56]. The aggregated representation is an useful benchmark to point out the effect of temporal correlations [54], and it allows to identify interesting properties of the system. For example, the observed super-linear relation between the degree and strength of an individual implies that on average highly-connected individuals spend more time in each interaction with respect to the poorly-connected ones [8, 16]. More in general, the strength of links and individuals helps not only to understand the structure of a social network, but also the dynamics of a wide range of phenomena involving human behavior, such as the formation of communities and the spreading of information and social influence [26, 46, 63]

A summary of the average properties of the datasets considered in this work is provided in Table I. The statistical and structural properties of the temporal networks representing SocioPatterns data have been extensively studied in the literature, see Refs. [16, 32, 54]. We will review them in the following sections, when performing a numerical comparison with the outcome of the proposed model.

| Dataset    | $N$ | $T$   | $\bar{p}$ | $\langle \Delta t \rangle$ | $\langle k \rangle$ | $\langle s \rangle$ |
|------------|-----|-------|-----------|----------------------------|---------------------|---------------------|
| Hospital   | 84  | 20338 | 0.049     | 2.67                       | 30                  | 0.0563              |
| Conference | 113 | 5093  | 0.060     | 2.13                       | 39                  | 0.0719              |
| School     | 126 | 5609  | 0.069     | 2.61                       | 27                  | 0.0808              |
| Congress   | 416 | 3834  | 0.075     | 2.96                       | 54                  | 0.131               |

TABLE I. Some properties of the SocioPatterns datasets under consideration:  $N$ , number of different individuals engaged in interactions;  $T$ , total duration of the contact sequence, in units of the elementary time interval  $t_0 = 20$  seconds;  $\bar{p}$ , average number of individuals interacting at each time step;  $\langle \Delta t \rangle$ , average duration of a contact;  $\langle k \rangle$  and  $\langle s \rangle$ : average degree and average strength of the projected network, aggregated over the whole sequence (see main text).

### III. A MODEL OF SOCIAL ATTRACTIVENESS

The model we propose is defined as follows [55]:  $N$  individuals, free to move in a closed environment, can interact between them when situated within a small distance (that we assimilate to the exchange range of the RFID devices). Agents perform a random walk of fixed step length  $v$  in a closed box of linear size  $L$  (corresponding to a density  $\rho = N/L^2$ ) and start interacting whenever they intercept another agent within a certain distance  $d$ . Crucially, each agent is characterized by an intrinsic “attractiveness” or social appeal, a consequence of their social status or the role they play in social gatherings, and which represents her power to raise interest in the others. The attractiveness  $a_i$  of each individual is randomly chosen from a given distribution  $\eta(a)$ , bounded in the interval  $a_i \in [0, 1]$ , which we choose to be uniform. Thus, when interacting, an individual either interrupts his motion to preserve an interaction, and this happens with a probability proportional to the attractiveness of the most interesting neighbor, or keeps moving. This translates into a walking probability  $p_i(t)$  of the agent  $i$  of the form

$$p_i(t) = 1 - \max_{j \in \mathcal{N}_i(t)} \{a_j\}, \quad (2)$$

where  $\mathcal{N}_i(t)$  is the set of neighbors of agent  $i$  at time  $t$ . Therefore, the more attractive an agent  $j$  is, the more interest she will raise in a neighbor agent  $i$ , who will slow down her random walk exploration accordingly.

Empirical data show that not all the agents are simultaneously present in the system, but they can be in an active state, moving and interacting, or in an inactive state, without moving nor interacting. To take this fact into consideration, each agent  $i$  in the model is further characterized by an activation probability  $r_i$ . At each time step, one inactive agent  $i$  can become active with a probability  $r_i$ , while one active and isolated agent  $j$  can become inactive with probability  $1 - r_j$ . We will choose the activation probability  $r_i$  of the agents randomly from an uniform distribution  $\phi(r)$ , bounded in  $r_i \in [0, 1]$ .

The results presented have been numerically simulated adopting the parameters  $v = d = 1$ ,  $L = 100$  and  $N =$

200, for a total duration  $T = 2 \times 10^4$  time steps, unless otherwise specified. In the initial conditions, agents are placed at randomly chosen positions, and are active with probability 1/2. Numerical results are averaged over  $10^2$  independent runs.

Before proceeding a comment is in order. We adopt here an operational definition of “attractiveness” as the property of an individual to attract the interest of other individuals, making them willing to engage in a conversation, or to listen to what he/she is saying. Thus, we do not enter in any speculations on what are the cultural or psychological factors that make a person attractive in this sense, but we reckon that many possible candidates exist, ranging from status [28] to extroversion [53]. In light of the success of our model in reproducing the empirical distributions (see below), we consider that identifying which feature, or set of features, the attractiveness is a proxy of represents one important direction for future work.

#### IV. INDIVIDUAL LEVEL DYNAMICS

In this section we compare the individual level predictions of the model against the observations from empirical data.

##### A. Temporal correlation

The temporal pattern of the individual contacts is one of the most distinctive feature of face-to-face interaction networks [16, 54], and in general of time-varying networks [41]. Relevant quantities measuring the correlation of this temporal pattern are [30]:

- the distribution of the duration  $\Delta t$  of the contacts between pairs of agents,  $P(\Delta t)$ ;
- the distribution of gap times  $\tau$  between two consecutive conversations involving a common individual,  $P(\tau)$ .

Empirical data reveal that both distributions are broad, with long tails that can be described in terms of a power-law function [16], reflecting the bursty nature of human interactions [6, 45]. Most contacts are short and separated by small amounts of time, but long interactions, as well as long inter-contact times, are always possible. Figure 1 shows that the model captures this property and quantitatively reproduces the phenomenology of the various datasets.

##### B. Time-aggregated networks

Additional information regarding the pattern of individual interactions is obtained by integrating the time-varying network into an aggregated weighted network.

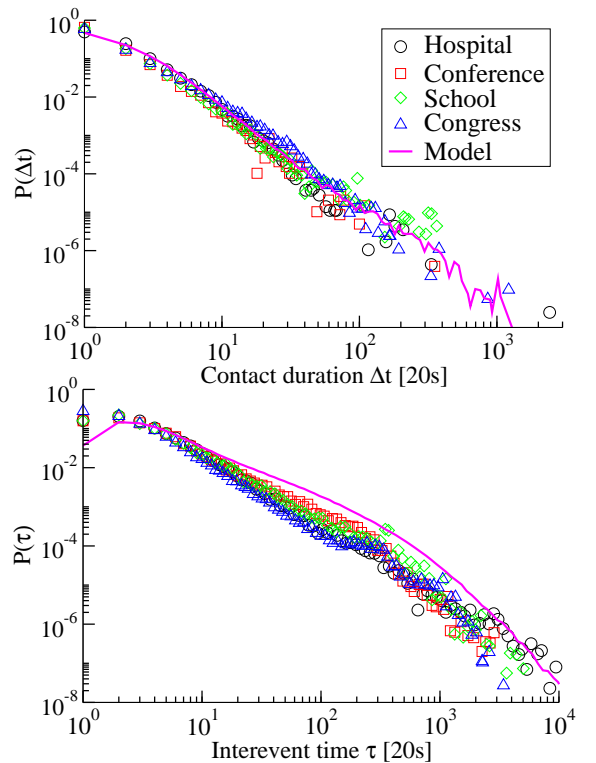


FIG. 1. (color online) **Burstiness of human contacts:** Distribution of the contact duration,  $P(\Delta t)$  (top) and the time interval between consecutive contacts,  $P(\tau)$ , (bottom) for various datasets (symbols) and for the attractiveness model (line).

As mentioned in section IIB, this corresponds to considering all the interactions occurring in a given time window  $\Delta t$  in the limit of  $\Delta t \rightarrow T$ , i.e. all the interactions taking place in the dataset. Repeated contacts between any two individuals  $i$  and  $j$  increase the weight  $w_{ij}$  associated to the link connecting them, and the sum of the weights of the links connecting an individual  $i$  to his peers (i.e. the total time  $i$  spends in conversations) represents the strength  $s_i$ .

In Fig. 2 we plot the distribution  $P(w)$  of weights  $w_{ij}$  between pairs of agents, and the cumulative distribution of the strength,  $P(s)$ , showing that the numerical simulation of the model are in excellent agreement with empirical data. The heavy tailed weight distribution,  $P(w)$ , shows that the heterogeneity in the duration of individual contacts persists even when interactions are accumulated over longer time intervals. The strength distribution  $P(s)$  has instead an exponential tail, as revealed by the cumulative distribution  $P_{\text{cum}}(s)$ , defined as the probability of finding any individual with a strength larger than  $s$ , see inset of Fig. 2. In both cases, our model leads to results that are fully compatible with the empirical evidence.

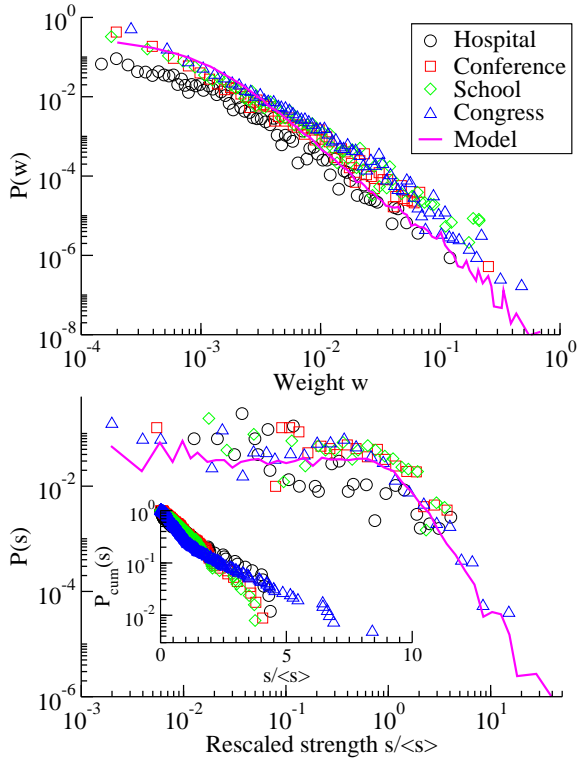


FIG. 2. (color online) **Time-integrated network:** Distribution of the weight,  $P(w)$ , (top) and rescaled strength,  $P(s)$  (bottom), for various datasets (symbols) and for the attractiveness model (line). In the inset we plot the cumulative strength distribution,  $P_{\text{cum}}(s)$ , to highlight the exponential decay of the  $P(s)$  (see Section VIII).

## V. GROUP LEVEL DYNAMICS

Another important aspect of human contact networks is the dynamics of group formation [4, 5], defined by a set of  $n$  individuals interacting simultaneously, not necessarily all with all, for a period of time  $\Delta t$ . As we have noted above, such groups play the important role of catalysts for decision making and problem solving [13]. In Fig. 3 (top) we plot the probability distribution of observing a group of size  $n$ ,  $P(n)$ , in any instant of the ongoing social event, for the different empirical data sets. The distributions are compatible with a power law behavior, whose exponent depends on the number of agents involved in the social event, with larger datasets (such for example the Congress one, see Table I) capable of forming bigger groups with respect to smaller data sets. Clearly, the model predictions are in substantial agreement with the data when we inform the model with a sensible, data-driven, value of  $N$ .

In order to explore the dynamics of group formation, we define the lifetime  $\Delta t$  of a group of size  $n$  as the time spent in interaction by the same set of  $n$  individuals, without any new arrival or departure of members of the group. In Fig. 3 (bottom) we plot the lifetime

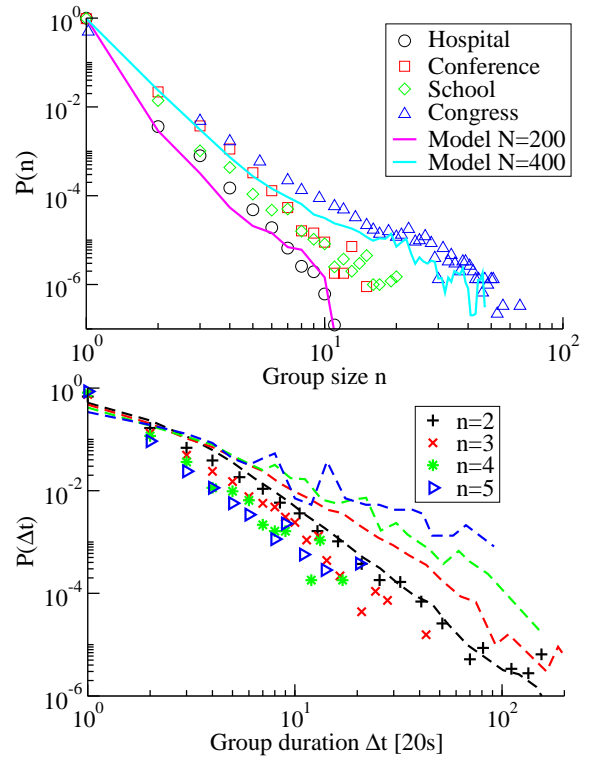


FIG. 3. (color online) **Group dynamics:** Up: Group size distribution  $P(n)$  for different datasets and for the model, numerically simulated with different number of agents  $N = 200$  and  $N = 400$ , and same size  $L = 100$ . Down: Lifetime distribution  $P_n(\Delta t)$  of groups of different size  $n$ , for the “Congress” dataset (symbols) and for the model numerically simulated with  $N = 400$  and  $L = 100$ . (dashed lines).

distribution  $P_n(\Delta t)$  of groups of different sizes  $n$ , finding that experimental and numerical results have a similar power-law behavior. We note however that for empirical data the lifetime distribution  $P_n(\Delta t)$  decays faster for larger groups, i.e. big groups are less stable than small ones, while the model outcome follows the opposite behavior. This means that, in the model, larger groups are (slightly) more stable than observed in the data. This is probably due to the fact that, the larger the group, the bigger the probability of finding two (or more) individuals with large attractiveness in the group, which guarantee the stability against departures. However, an alternative explanation could be that the RFID devices of the SocioPatterns experiment require individuals to face each others within a given angle, making the group definition effectively more fragile than in the model, where such directionality is absent.

## VI. COLLECTIVE LEVEL DYNAMICS AND SEARCHING EFFICIENCY

The temporal dimension of any time-varying graph has a deep influence on the dynamical processes taking place

upon such structures [41]. In the fundamental example of opinion (or epidemic) spreading, for example, the time at which the links connecting an informed (or infected) individual to his neighbors appear determines whether the information (or infection) will or will not be transmitted. In the same way, it is possible that a process initiated by individual  $i$  will reach individual  $j$  through an intermediate agent  $k$  through the path  $i \rightarrow k \rightarrow j$  even though a direct connection between  $i$  and  $j$  is established later on. This information is lost in the time aggregated representation of the network, where any two neighboring nodes are equivalent [30]. In general, time respecting paths [29] determine the set of possible causal interactions between the agents of the graph, and the state of any node  $i$  depends on the state of any other vertex  $j$  through the collective dynamics determining their causal relationship.

For any two vertices, we can measure the shortest time-respecting path,  $l_{ij}^s$ , and fastest time-respecting path,  $l_{ij}^f$ , between them [54]. The former is defined as the path with the smallest number of intermediate steps between nodes  $i$  and  $j$ , and the latter is the path which allows to reach  $j$  starting from  $i$  within the smallest amount of time. In Fig. 4 we plot the probability distributions of the shortest and fastest time-respecting path length,  $P_s(l)$  and  $P_f(l)$ , respectively, of both empirical data and model, finding that they show a similar behavior, decaying exponentially, and being peaked for a small number of steps.

Given the importance of causal relationship on any spreading dynamics, it is interesting to explicitly address the dynamical unfolding of a diffusive process. Here we analyze the simplest example of a search process, the random walk, which describes a walker traveling the network and, at each time step, selecting randomly its destination among the available neighbors of the node it occupies. The random walk represents a fundamental reference point for the behavior of any other diffusive dynamics on a network, when only local information is available. Indeed, assuming that each individual knows only about the information stored in each of its nearest neighbors, the most naive economical strategy is the random walk search, in which the source vertex sends one message to a randomly selected nearest neighbor [3]. If that individual has the information requested, it retrieves it; otherwise, it sends a message to one of its nearest neighbors, until the message arrives to its final target destination. In this context, a quantity of interest is the probability that the random walk actually find its target individual  $i$  at any time in the contact sequence,  $P_r(i)$ , or *global reachability* [41, 54].

In principle, the reachability of an individual  $i$  must be correlated with the total time spent in interactions, namely his strength  $s_i$ , but it also depends on the features of the considered social event, such as the density of the interaction  $\bar{p}$ , the total duration  $T$  and possibly other event-specific characteristic (see Table I for information of the different data sets considered). On the basis of

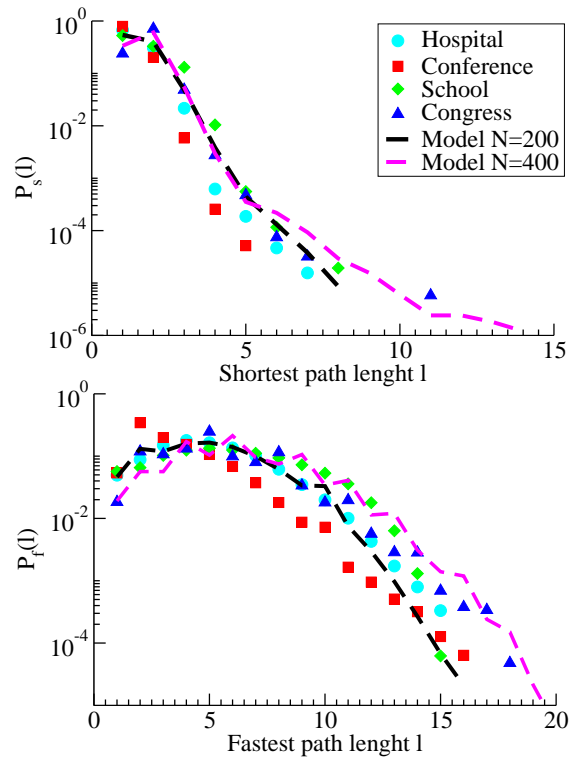


FIG. 4. (color online) **Time-respecting paths:** Probability distributions of the shortest,  $P_s(l)$ , (top) and fastest,  $P_f(l)$ , (bottom) path length, for the time-varying network obtained by the empirical data and by the model, numerically simulated with different number of agents  $N = 200$  and  $N = 400$ , and same size  $L = 100$ .

a simple mean field argument, it has been shown [54] that the probability of node  $i$  to be reached by the random walk,  $P_r(i)$ , is correlated with its relative strength  $s_i/\langle s \rangle N$ , times the average number of interacting individuals at each time step,  $\bar{p}T$ . In Fig 5 we plot the reachability  $P_r(i)$  against the rescaled strength  $s_i\bar{p}T/\langle s \rangle N$ , showing that very different empirical data sets collapse into a similar functional form. Remarkably, the model is able to capture such behavior, with a variability, also found in the data, which depends on the density  $\rho$  of the agents involved. As noted for the group dynamics, a larger density corresponds to a higher reachability of the individuals. We note that the empirical data are reproduced by the model for the same range of density considered in the previous analysis.

## VII. MODEL ROBUSTNESS

The model discussed above depends on different numerical and functional parameters, namely the individual density  $\rho$ , the attractiveness distribution  $\eta(a)$  and the activation probability distribution  $\phi(r)$ . As we have seen, some properties of the model, especially those related to group and collective level dynamics, do indeed

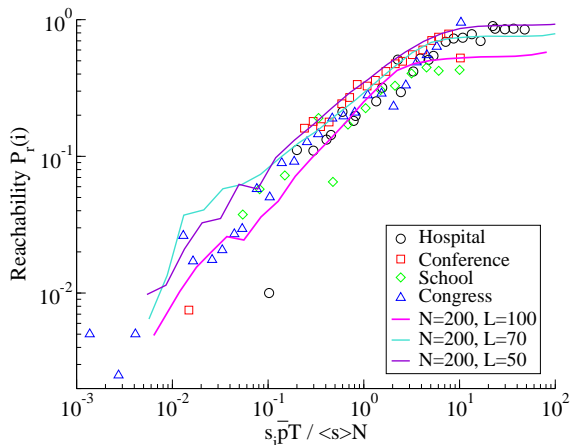


FIG. 5. (color online) **Reachability:** Correlation between the reachability of agent  $i$ ,  $P_r(i)$ , and his rescaled strength,  $s_i \bar{p} T / \langle s \rangle N$ . The empirical data sets considered (symbols) and the model (lines), numerically simulated with different density  $\rho$ , follow a close behavior. We averaged the reachability of each individual over at least  $10^2$  different runs, starting with different source node.

depend of the density  $\rho$  (or the number of individuals  $N$ ), in such a way that model is able to reproduce empirical data only when fed with a value of  $N$  corresponding to the data set under consideration. The model properties relevant to the individual level dynamics however, such as the contact duration and weight distributions,  $P(\Delta t)$  and  $P(w)$ , do not change in a reasonable range of density. In Fig. 6 one can observe that the functional form of these distributions is robust with respect to changes of the individual density, supporting the natural notion that individual level dynamics is mainly determined by close contacts of pairs of individuals, and rather independent of eventual multiple contacts, which become rarer for smaller densities.

We have also explored the dependence of the model on the activation probability distribution and the walking probability. In particular, instead of a uniform activation probability distribution, we have considered a constant distribution

$$\phi(r) = \delta_{r,r_0}, \quad (3)$$

where  $\delta_{r,r'}$  is the Kronecker symbol. As we can see from Fig. 6 the output of the model is robust with respect to changes of this functional parameter.

Finally, in the definition of the model we have adopted the simplest motion dynamics for individuals, namely an isotropic random walk in which the distance  $v$  covered by the agents at each step is constant and arbitrarily fixed to  $v = 1$ . However, it has been noted for long that a Lévy flight turns out to provide a better characterization of human or animal movement and foraging [61]. In this case, the random walk is still isotropic, but now the distance covered in each step is a random variable, extracted

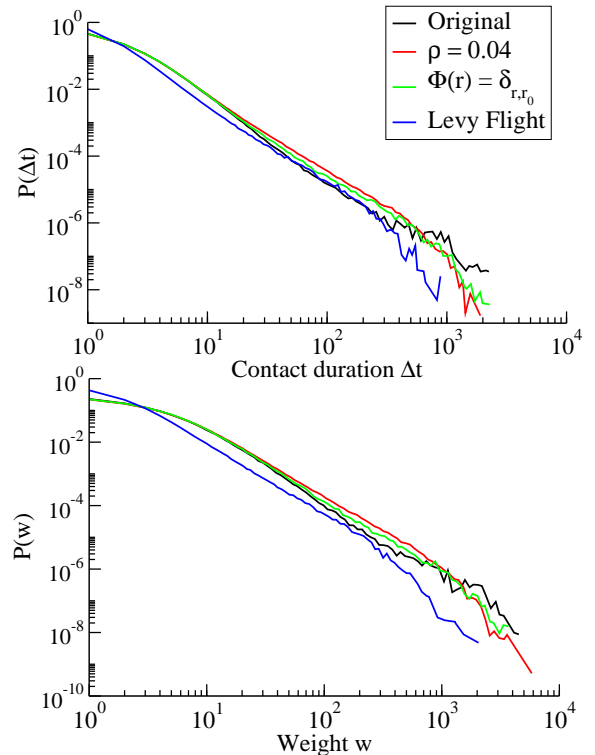


FIG. 6. (color online) **Robustness:** Contact duration (top) and weigh (bottom) probability distributions obtained by simulating the model in its original definition, with a different density  $\rho$  given by  $N = 400$  individuals, with constant activation probability  $\Phi(r) = \delta_{r,r_0}$  with  $r_0 = 0.5$ , and with a Lévy flight motion dynamics, obtained by using Eq. 4 with  $\gamma = 2.5$  for extracting the step length.

from a probability distribution

$$\mathcal{L}(v) \simeq v^{-\gamma}, \quad (4)$$

with a long tailed form. In Fig. 6 we show that adopting a Lévy flight motion dynamics gives rise to outcomes in very good agreement with the original definition of the model. We note, however, that the step length probability distribution  $\mathcal{L}(v)$  has a natural cutoff given by the size of the box where the agents move,  $v < L$ , reducing the degree of heterogeneity that the walk can cover.

## VIII. DISCUSSION

Understanding the temporal and structural properties of human contact networks has important consequences for social sciences, cognitive sciences, and epidemiology. The interest in this area is not new, but has been fueled by the recent availability of large amounts of empirical data, obtained from expressly designed experimental setups. The universal features observed in these empirical studies prompt for the design of general models, capable of accounting for the observed statistical regularities.

In this paper we reported the results obtained from a simple model in which individuals perform a random walk and start interactions based on a close proximity rule. The key ingredient is the social attractiveness of the individuals, which has the effect of slowing down the random walk performed by the agents and determines the duration of their interactions. By means of numerical simulations, we observed that the model reproduces the results obtained from the empirical analysis of the human contact networks provided by the SocioPatterns collaboration [1]. The match between the model and the empirical results is independent of the numerical and functional form of the diverse parameters defining the model. However, the attractiveness distribution  $\eta(a)$  used in the model definition deserves a more detailed discussion. Its functional form is hard to access empirically, and it is likely to be in its turn the combination of different elements, such as prestige, status, role, etc. Moreover, even though in general attractiveness is a relational variable – the same individual exerting different interest on different agents – we have assumed the simplest case of a uniform distribution for the attractiveness. For this reason it is important to stress some facts that support our decision, and to investigate the effect of the attractiveness distribution on the model outcome.

The choice of a uniform  $\eta(a)$  is dictated by the maximum entropy principle, according to which the best guess for a unknown but bounded distribution (as the attractiveness distribution has to be, if we want it to represent a probability) is precisely the uniform distribution. However, we can also explore the relation between the attractiveness and some other variables that can be accessed empirically. In particular, the attractiveness of one individual and the strength of the corresponding node of the integrated network are expected to be (non-trivially) related, since the more attractive an individual is, the longer the other agents will try to engage him in interactions. Fig. 2 shows that the strength distribution  $P(s)$  of the time-integrated network obtained from the empirical data, which follows approximately an exponential behavior, is well fitted by the model. Thus, if we hypothesize that the attractiveness and strength probability distributions are related as  $P(s)ds \sim \eta(a)da$ , with  $\eta(a)$  uniform in  $[0,1]$ , it follows that the strength of an individual should depend on his attractiveness as

$$s(a) \sim -\log(1-a). \quad (5)$$

We find that this relation is fulfilled by the model (data not shown), showing that in the model the time spent in interactions by the individuals is directly related with their degree of attractiveness. Therefore the guess of a heterogeneous but uniform  $\eta(a)$  leads to an exponential decay of the  $P(s)$  for the model, in accordance with experimental data, and providing grounds to justify this choice of attractiveness distribution. Moreover, the simple relation expressed by Eq. 5 may suggest a way to validate the model, once some reliable measure of attractiveness will be available.

Finally, it is worth highlighting that the form of the attractiveness distribution  $\eta(a)$  is crucial for the model outcome. Therefore, it is interesting to explore the effect of different functional forms of  $\eta(a)$ , for example incorporating a higher degree of heterogeneity, such as in the case of a power-law distribution. We note, however, that the form of Eq. (2) imposes to the  $a_i$  variable to be a probability, with the consequent constraint of being bounded,  $a_i \in [0,1]$ . A power law distribution defined over a bounded support presents some issues, such as the necessity of imposing a lower bound to prevent divergence close to 0. To avoid this inconvenient, one can redefine the motion rule of Eq. (2) as

$$p_i^{\text{inv}}(t) = \frac{1}{\max_{j \in \mathcal{N}_i(t)} \{a'_j\}}, \quad (6)$$

with the new attractiveness variable  $a'_i$  unbounded,  $a'_i \in [1, \infty)$ . If we impose the walking probability of Eqs. (2) and (6) to be the same, and we use the relation  $\eta(a)da = \zeta(a')da'$ , we find that the new attractiveness distribution  $\zeta(a')$  has the form of a power law,  $\zeta(a') = (\gamma - 1)a'^{-\gamma}$ , with exponent  $\gamma = 2$ . Therefore, assuming a motion rule of the form of Eq. (6), a power law attractiveness distribution will give rise to same model results, as confirmed by numerical simulations (data not shown).

On the same line of argument, it would be interesting to relate the agents' activation probability,  $r_i$ , with some empirically accessible properties of the individuals. Unfortunately, finding the activation probability distribution  $\phi(r)$  is a hard task with the information contained in the available datasets. In the face-to-face interaction deployment, indeed, a non-interacting but active individual is indistinguishable from an inactive individual who is temporary not involved into the event. Thus, simply measuring probability to be not involved in a conversation does not inform on the  $\phi(r)$ , but instead considers something more related with the burstiness of the individual activity. In any case, however, the model behavior is independent of the functional form the activation distribution, so that this point is less crucial.

In summary, we showed that a simple model based on the concept of social attractiveness is able to account for the main statistical properties of human contact networks at different scales. This finding prompts for further empirical research, based on more detailed and extensive experimental setups, which can shed light on the role of this attractiveness. Such research would help to further refine and validate the model considered here, and could potentially provide new insights for the social and cognitive sciences.

## IX. ACKNOWLEDGMENTS

We acknowledge financial support from the Spanish MEC, under project FIS2010-21781-C02-01, and EC FET-Proactive Project MULTIPLEX (Grant No. 317532). We thank the SocioPatterns collaboration



for providing privileged access to datasets “Hospital”,

“School”, and “Congress”. Dataset “Conference” is publicly available at [1].

- 
- [1] <http://www.sociopatterns.org>.
- [2] L. A. Adamic and N. Glance. The political blogosphere and the 2004 us election: divided they blog. In *Proceedings of the 3rd international workshop on Link discovery*, pages 36–43. ACM, 2005.
- [3] L. A. Adamic, R. M. Lukose, A. R. Puniyani, and B. A. Huberman. Search in power-law networks. *Phys. Rev. E*, 64:046135, Sep 2001.
- [4] H. Arrow, J. E. McGrath, and J. L. Berdahl. *Small groups as complex systems: Formation, coordination, development, and adaptation*. Sage Publications, 2000.
- [5] R. F. Bales. Interaction process analysis; a method for the study of small groups. 1950.
- [6] A.-L. Barabasi. The origin of bursts and heavy tails in human dynamics. *Nature*, 435:207, 2005.
- [7] A.-L. Barabási. *Bursts: The Hidden Patterns Behind Everything We Do, from Your E-mail to Bloody Crusades*. Penguin. com, 2010.
- [8] A. Baronchelli, R. Ferrer-i Cancho, R. Pastor-Satorras, N. Chater, and M. H. Christiansen. Networks in cognitive science. *Trends in cognitive sciences*, 17(7):348–360, 2013.
- [9] A. Baronchelli and F. Radicchi. Lévy flights in human behavior and cognition. *Chaos, Solitons & Fractals*, 56:101–105, 2013.
- [10] W. R. Bion. *Experiences in groups: And other papers*. Routledge, 2013.
- [11] C. Bird, A. Gourley, P. Devanbu, M. Gertz, and A. Swaminathan. Mining email social networks. In *Proceedings of the 2006 international workshop on Mining software repositories*, pages 137–143. ACM, 2006.
- [12] D. Brockmann, L. Hufnagel, and T. Geisel. The scaling laws of human travel. *Nature*, 439(7075):462–465, 2006.
- [13] M. Buchanan. *The social atom*. Bloomsbury, New York, NY, USA, 2007.
- [14] K. Carley. A theory of group stability. *American Sociological Review*, pages 331–354, 1991.
- [15] D. P. Carpenter, K. M. Esterling, and D. M. Lazer. Friends, brokers, and transitivity: Who informs whom in washington politics? *Journal of Politics*, 66(1):224–246, 2004.
- [16] C. Cattuto, W. Van den Broeck, A. Barrat, V. Colizza, J.-F. Pinton, and A. Vespignani. Dynamics of person-to-person interactions from distributed rfid sensor networks. *PLoS ONE*, 5:e11596, 2010.
- [17] D. Centola. The spread of behavior in an online social network experiment. *science*, 329(5996):1194–1197, 2010.
- [18] H. H. Clark and S. E. Brennan. Grounding in communication. *Perspectives on socially shared cognition*, 13(1991):127–149, 1991.
- [19] W. V. den Broeck, C. Cattuto, A. Barrat, M. Szomsor, G. Correndo, and H. Alani. The live social semantics application: a platform for integrating face-to-face presence with on-line social networking. In *Proceedings of the 8th Annual IEEE International Conference on Pervasive Computing and Communications*, page 226, 2010.
- [20] G. Doherty-Sneddon, A. Anderson, C. O’Malley, S. Langton, S. Garrod, and V. Bruce. Face-to-face and video-mediated communication: A comparison of dialogue structure and task performance. *Journal of Experimental Psychology: Applied*, 3(2):105, 1997.
- [21] P. Doreian, R. Kapuscinski, D. Krackhardt, and J. Szczygula. A brief history of balance through time. *Journal of Mathematical Sociology*, 21(1-2):113–131, 1996.
- [22] N. Eagle, A. S. Pentland, and D. Lazer. Inferring friendship network structure by using mobile phone data. *Proceedings of the National Academy of Sciences*, 106(36):15274–15278, 2009.
- [23] N. B. Ellison, C. Steinfield, and C. Lampe. *Journal of Computer-Mediated Communication*, 12(4):1143–1168, 2007.
- [24] M. C. Gonzalez, C. A. Hidalgo, and A.-L. Barabasi. Understanding individual human mobility patterns. *Nature*, 453(7196):779–782, 2008.
- [25] M. S. Granovetter. The strength of weak ties. *American journal of sociology*, pages 1360–1380, 1973.
- [26] A. L. Hill, D. G. Rand, M. A. Nowak, and N. A. Christakis. Infectious disease modeling of social contagion in networks. *PLoS computational biology*, 6(11):e1000968, 2010.
- [27] J. Hollan and S. Stornetta. Beyond being there. In *Proceedings of the SIGCHI conference on Human factors in computing systems*, pages 119–125. ACM, 1992.
- [28] A. B. Hollingshead. Four factor index of social status. *Unpublished*, 1975.
- [29] P. Holme. Network reachability of real-world contact sequences. *Phys. Rev. E*, 71:046119, Apr 2005.
- [30] P. Holme and J. Saramäki. Temporal networks. *Physics Reports*, 519:97–125, 2012.
- [31] B. A. Huberman, D. M. Romero, and F. Wu. Social networks that matter: Twitter under the microscope, 2008. arxiv:0812.1045.
- [32] L. Isella, J. Stehlé, A. Barrat, C. Cattuto, J. Pinton, and W. Van den Broeck. What’s in a crowd? analysis of face-to-face behavioral networks. *J. Theor. Biol.*, 271(1):166–180, 2011.
- [33] M. Jackson. *Social and economic networks*. Princeton University Press, 2010.
- [34] S. Kiesler, J. Siegel, and T. W. McGuire. Social psychological aspects of computer-mediated communication. *American psychologist*, 39(10):1123, 1984.
- [35] H. Kwak, C. Lee, H. Park, and S. Moon. What is twitter, a social network or a news media? In *Proceedings of the 19th international conference on World wide web*, pages 591–600. ACM, 2010.
- [36] D. Lazer. Networks in political science: Back to the future. *PS: Political Science & Politics*, 44(01):61–68, 2011.
- [37] D. Lazer, A. S. Pentland, L. Adamic, S. Aral, A. L. Barabasi, D. Brewer, N. Christakis, N. Contractor, J. Fowler, M. Gutmann, et al. Life in the network: the coming age of computational social science. *Science (New York, NY)*, 323(5915):721, 2009.

- [38] F. Liljeros, C. R. Edling, L. A. N. Amaral, H. E. Stanley, and Y. Åberg. The web of human sexual contacts. *Nature*, 411(6840):907–908, 2001.
- [39] P. V. Marsden. Core discussion networks of americans. *American sociological review*, pages 122–131, 1987.
- [40] D. Mocanu, A. Baronchelli, N. Perra, B. Gonçalves, Q. Zhang, and A. Vespignani. The twitter of babel: Mapping world languages through microblogging platforms. *PLoS one*, 8(4):e61981, 2013.
- [41] J. Moody. The importance of relationship timing for diffusion. *Social Forces*, 81(1):25–56, 2002.
- [42] B. A. Nardi and S. Whittaker. The place of face-to-face communication in distributed work. *Distributed work*, pages 83–110, 2002.
- [43] M. E. J. Newman. *Networks: An introduction*. Oxford University Press, Oxford, 2010.
- [44] N. Nohria and R. Eccles. Face-to-face: Making network organizations work. *Technology, Organizations and Innovation: Critical Perspectives on Business and Management*, pages 1659–1681, 2000.
- [45] J. G. Oliveira and A.-L. Barabasi. Human dynamics: Darwin and einstein correspondence patterns. *Nature*, 437(7063):1251–1251, 10 2005.
- [46] J.-P. Onnela, J. Saramäki, J. Hyvönen, G. Szabó, D. Lazer, K. Kaski, J. Kertész, and A.-L. Barabási. Structure and tie strengths in mobile communication networks. *Proceedings of the National Academy of Sciences*, 104(18):7332–7336, 2007.
- [47] N. Perra, A. Baronchelli, D. Mocanu, B. Gonçalves, R. Pastor-Satorras, and A. Vespignani. Random walks and search in time-varying networks. *Physical Review Letters*, 109(23):238701, 2012.
- [48] T. Preis, H. S. Moat, and H. E. Stanley. Quantifying trading behavior in financial markets using google trends. *Scientific reports*, 3, 2013.
- [49] F. Radicchi, A. Baronchelli, and L. A. Amaral. Rationality, irrationality and escalating behavior in lowest unique bid auctions. *PloS one*, 7(1):e29910, 2012.
- [50] I. Rhee, M. Shin, S. Hong, K. Lee, S. J. Kim, and S. Chong. On the levy-walk nature of human mobility. *IEEE/ACM Transactions on Networking (TON)*, 19(3):630–643, 2011.
- [51] B. Ribeiro, N. Perra, and A. Baronchelli. Quantifying the effect of temporal resolution on time-varying networks. *Scientific reports*, 3, 2013.
- [52] M. Salathé, M. Kazandjieva, J. W. Lee, P. Levis, M. W. Feldman, and J. H. Jones. A high-resolution human contact network for infectious disease transmission. *Proceedings of the National Academy of Sciences*, 107(51):22020–22025, 2010.
- [53] K. R. Scherer. Personality inference from voice quality: The loud voice of extroversion. *European Journal of Social Psychology*, 8(4):467–487, 1978.
- [54] M. Starnini, A. Baronchelli, A. Barrat, and R. Pastor-Satorras. Random walks on temporal networks. *Phys. Rev. E*, 85:056115, May 2012.
- [55] M. Starnini, A. Baronchelli, and R. Pastor-Satorras. Modeling human dynamics of face-to-face interaction networks. *Phys. Rev. Lett.*, 110:168701, Apr 2013.
- [56] J. Stehlé, N. Voirin, A. Barrat, C. Cattuto, L. Isella, J.-F. Pinton, M. Quaggiotto, W. Van den Broeck, C. Régis, B. Lina, and P. Vanhems. High-resolution measurements of face-to-face contact patterns in a primary school. *PLoS ONE*, 6(8):e23176, 08 2011.
- [57] A. Stopczynski, V. Sekara, P. Sapiezynski, A. Cuttone, J. E. Larsen, and S. Lehmann. Measuring large-scale social networks with high resolution. *PLOS One*, 9(4):e95978, 2014.
- [58] M. Storper and A. J. Venables. Buzz: face-to-face contact and the urban economy. *Journal of economic geography*, 4(4):351–370, 2004.
- [59] Y. Takhteyev, A. Gruzd, and B. Wellman. Geography of twitter networks. *Social networks*, 34(1):73–81, 2012.
- [60] R. Toivonen, L. Kovanen, M. Kivelä, J.-P. Onnela, J. Saramäki, and K. Kaski. A comparative study of social network models: Network evolution models and nodal attribute models. *Social Networks*, 31(4):240–254, 2009.
- [61] G. Viswanathan, M. da Luz, E. Raposo, and H. Stanley. *The Physics of Foraging: An Introduction to Random Searches and Biological Encounters*. Cambridge University Press, Cambridge, 2011.
- [62] S. Wasserman. *Social network analysis: Methods and applications*, volume 8. Cambridge university press, 1994.
- [63] D. J. Watts. A twenty-first century science. *Nature*, 445(7127):489–489, 2007.
- [64] B. Wellman and S. Wortley. Different strokes from different folks: Community ties and social support. *American journal of Sociology*, pages 558–588, 1990.
- [65] K. Zhao, J. Stehlé, G. Bianconi, and A. Barrat. Social network dynamics of face-to-face interactions. *Physical Review E*, 83(5):056109, 2011.